Design, Synthesis and Characterization of Porous Organic Frameworks

[a]R. Zafar, [b]M. Maqbool and [a]S. Shabbir
[a]Department of Materials and Engineering, Institute of Space Technology, Islamabad, Pakistan
[b]IRCBM, COMSATS Institute of Information Technology, Lahore, Pakistan

Abstract— **Here we present the synthesis of porous organic frameworks (POFs) through a single-pot, low temperature, metal free, facile condensation polymerization reaction between a triacid chloride and a diamine, thus producing POFs decorated internally with amide linkages and externally with acid and amine groups that are readily available for further functionalization. Relative molar concentrations of reactants were chosen as representative parameters to monitor morphology and end groups. POFs were analyzed by FTIR, SEM, TGA and BET analyses. A higher thermal stability was acquired due to the presence of amide linkages in the polymer backbone. Porosity evaluated by BET studies demonstrated an average pore size and surface area of 32.8 nm and 0.6503 m²/g, respectively.**

***Key words*— POFs; SEM; FTIR; TGA.**

I. Introduction

Polymeric organic frameworks (POFs) are categorized as porous functional materials with large surface area and light weight [1]. They find immense applications in the field of gas capture and storage technologies, for instance, CO_2 from flue gases and H_2 for fuel cells in the aerospace industry [2-3]. In pure porous organic polymers, covalent bonds are continuous in the entire structure thus rendering a high physical and chemical stability in harsh environments and a pronounced surface area. This surface area is comparable to metal organic frameworks (MOFs) [4]. POFs are an emerging class of extremely lightweight [5], hyper-cross-linked polymer networks [4, 6], incorporated with pure organic entities [7], tunable pore size [8] and functionalized internal surfaces [9].

In this regard, the synthesis of tunable porous materials necessitates a facile approach which must meet the design objectives in terms of efficiency, energy demands, recharge kinetics, size, availability, cost of process technologies and safety measures required for their ease of utility and portability at the application sites and systems.

The targeted design is to explore a facile route to synthesize POFs and tune their end functionality ultimately controlling their porosity. Hence, three POFs were fabricated by varying the stoichiometry of the monomers. The synthesized samples were investigated using FTIR, TGA, BET and SEM techniques.

II. Experimental Details

A. Chemical Reagents

1,3,5-Benzenetricarbonyl trihloride (BTC, Mw:265.48, Purity 98%), 4,4′ Oxydianiline (ODA, Mw:200.24, Purity 97%) and N,N-Dimethylacetamide (DMAc, Mw:87.12, Purity 99.8%) were purchased from Sigma Aldrich.

B. Synthesis of Porous Organic Network

Polyamide networks were synthesized by adding aromatic monomers of diamine and triiacid chloride via solution polymerization route. A resealable conical flask, equipped with magnetic stirrer, was charged with BTC in 10ml DMAc and ODA in 10ml DMAc separately. The molar ratios of BTC and ODA were 1:1, 2:1and 3:2 for sub-systems A-1, A-2 and A-3, respectively (Table 1).

The flasks were sealed and stirred for about 1 hour. After complete dissolution of diamine in DMAc a triacid chloride solution was poured into diamine solution for gel formation. 3-D growth of polyamide network via condensation polymerization was achieved within seconds without stirring at 25 ^{o}C.

Amide linkages were formed as confirmed by FTIR spectroscopy. Two functionalities were utilized for polymer formation, an amine functionality and an acid chloride functionality to form an amide linkage which constitutes an internal decor of the POF framework.

Both the amine and acid chloride groups were optimized to be retrained on the polymeric outer structure to form the external decor of the framework. The amide group can act as a preferential adsorption site for the CO_2 capture.

Table 1 - Summary of synthesis parameters

POF System	Sub-systems	Molar ratios of Monomer used		End Group
		BTC	ODA	
A	A-1	1	1	-COOH
	A-2	1	2	$-NH_2$
	A-3	3	2	-COOH

C. Measurements

Chemical stability of the synthesized POFs was determined qualitatively by adding 10 mg of the polyamide network in 1 mL of solvent or dilute solutions of acids and bases at room temperature. FTIR spectra were recorded at room temperature using Nicolet FTIR Spectrometer at a resolution of 4 cm^{-1}. Thermal stability of the POFs was measured using METTLER TOLEDO TGA/SDTA 851^e thermo gravimetric analyzer. The effect of temperature was investigated by taking 8–12 mg of the dried POF sample in Al_2O_3 crucible heated from 25 to 1000 °C at a ramping rate of 10 °C/min under nitrogen flux of 50 mL/min. BET method was employed using nitrogen bearing molecular cross-sectional area of 0.162 nm². Dried POFs were ground to a fine powder for surface area analysis and degassed under vacuum for 6 hours. POFs were analyzed for N_2 gas adsorption and their surface area was evaluated at 77K and relative pressure range $P/P_o \approx$ 0.2-0.9.

III. Results and Discussion

A. Chemical Stability Test

Stability tests for POFs are crucial for estimating their their working life. In practical applications, POFs are exposed to different environmental conditions such as corrosive environment, acidic, basic and neutral media in their immediate vicinity. A-1, A-2 and A-3 were found to be stable in organic solvents and a wide range of acidic and basic media. Rigid amide structure of POFs stabilizes in corrosive environment. Table 2 summarizes the stability of POFs in different media.

Table 2.

Chemical stability results under different media

Systems	DMSO	Water	Ethanol	Dilute HNO_3	Dilute H_2SO_4	NaOH (0.1 M)	U-V radiations
A-1	Partially Stable	Stable	Stable	Turbidity POFs stable	Turbidity POFs stable	Stable	No effect
A-2	Partially Stable	Stable	Stable	Turbidity POFs stable	Turbidity POFs stable	Stable	No effect
A-3	Partially Stable	Stable	Stable	Turbidity POFs stable	Turbidity POFs stable	Stable	No effect

B. FTIR Spectroscopy

FTIR spectrographs are shown in Fig. 1. FTIR spectroscopy confirmed the presence of terminal acid C=O, amide N-H and amide C=O linkages in the polymer networks. The presence of C-H stretches above 3000 cm^{-1} indicated the presence of aromatic moieties in POFs. All the spectra depicted the stretching vibration of amide N-H bond at 3400 cm^{-1}. The characteristic for hydrogen bonding broadband transmittance peak due to amide N-H between 3600-3300 cm^{-1} was present in systems A-2 and A-3, hence, a true indication of H-bonding in these POFs. The FTIR spectra for various POFs samples confirmed the presence of acidic carbonyl group as end functionality in systems A-1 at 1736 cm^{-1} and A-3 at 1715 cm^{-1}. N-H bending peaks for A-2 at 1606 cm^{-1} confirmed the presence of $-NH_2$ end functional group. C=O stretches and N-H bending peaks for amide confirmed the formation of the amide linkage in all the systems. Scheme for the synthesis of three families of POFs are shown in Fig. 2. The optimization of end functional groups by varying relative molar ratios of monomers was found to be successful and has been verified by FTIR spectra.

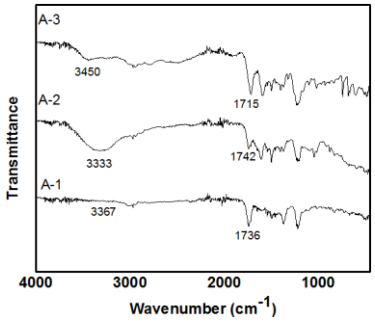

Fig. 1. FTIR spectra of various POF samples

Table 3.
Comparison of FTIR data for various functional groups

Functional Group	A-1	A-2	A-3
N-H Stretch	3367	3333	3450
Aromatic C-H Stretch	2970	2970	2969
C=O stretch (Acid)	1736	-	1715
C=O stretch (Amide)	1646	1742	-
N-H bending(Amide)	1558	1540	1592
Amine N-H bending	-	1606	-
Aromatic C=C stretch	1496	1456	1496
C–H in-plane bending	1106	1216	1288
Aromatic C-H “oop" band	829	825	738

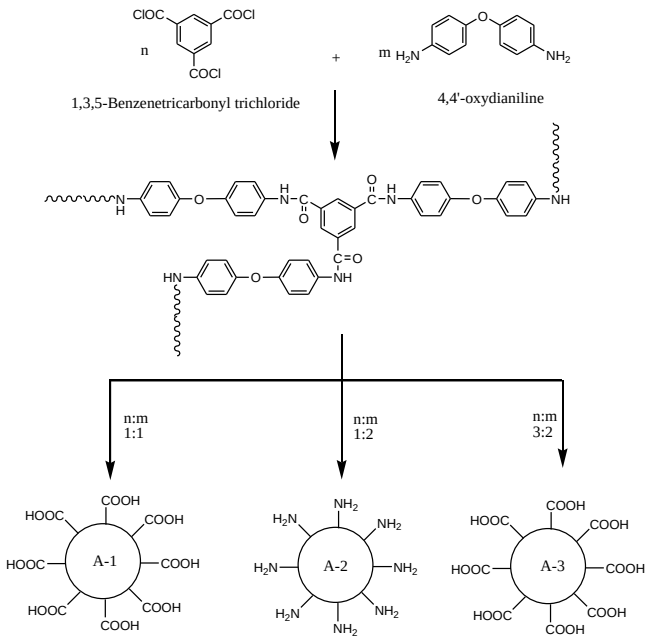

Fig. 2. Scheme for the synthesis of POF system-A

C. Morphological Studies

Figs. 3, 4 and 5 show the SEM images for the POF system-A in which ODA and BTC were used as initial precursors in a molar ratio of 1:1, 2:1 and 3:2, respectively. Fig. 3 for system A-1, depicts the characteristic surface impregnated with polyamide matrix material with no obvious porosity.

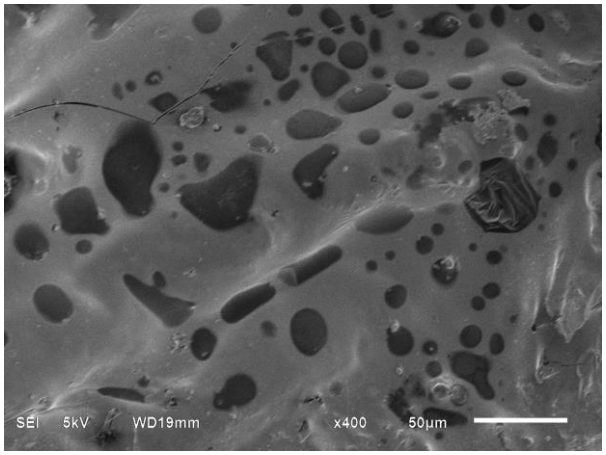

Fig. 3. SEM micrograpgh of sub-system A-1

Fig. 4 demostrates the surface features of mixed morphology of particulates fitted into intervening spaces giving rise to an efficiently packed, solid matrix system for sample A-2.

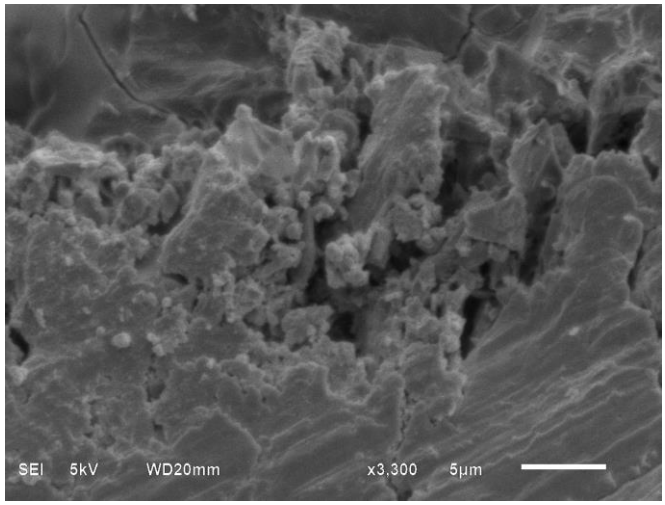

Fig. 4. SEM micrograpgh of sub-system A-2

Figs. 5-A and 5-B display the surface morphology of sub-system A-3 where bigger particulates seemed to be embedded in polyamide matrix material. An agglomeration of monolithic microglobules, ranging in size from 1-10 µm, were seen in the microstructure. The presence of microglobules can be explained by the robust formation of crystalline polyamides accompanied by thermal evaporation of network structures. Highly exothermic reaction at the time of gelation gave rise to thermally evaporated crystalline polyamides. Moreover, higher degree of crstallinity was confirmed by the TGA curve for this system. These crystalline materials might have porosity but it was not obvious. Such materials may possess intrinsic porosity which can be studied by X-ray crystallography [10] in detail. However, these materials with less density can open new horizons of research for robust crystalline polymer synthesis, which do not have extrinsic porosity. Similar structures have been reported in literature using ring opening metathesis reactions [11], which made use of optimized experimental

conditions, use of porogens and complex coordination chemistries [12].

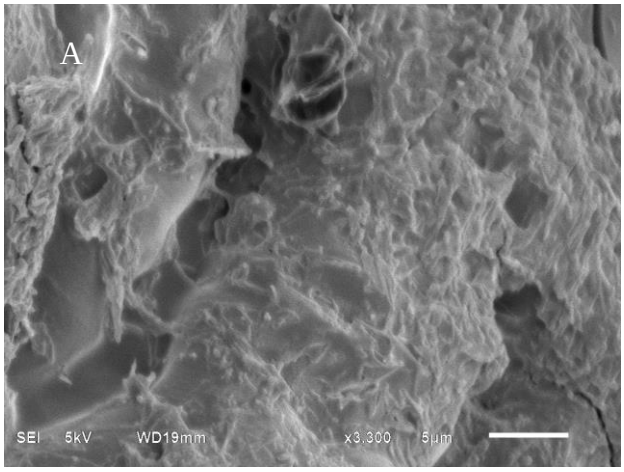

Fig. 5A. SEM micrograpghs of sub-system A-3

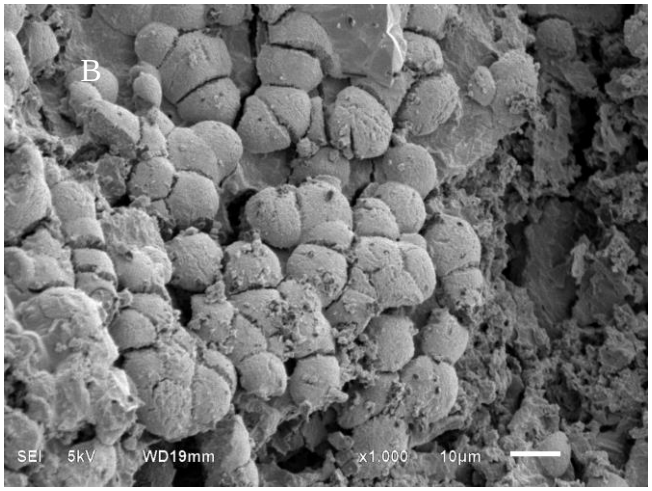

Fig. 5B. SEM micrograpghs of sub-system A-3

D.Thermogravimetric Analysis

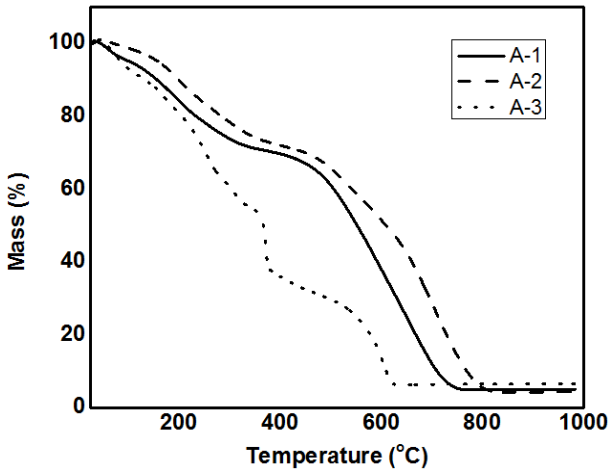

Fig. 6. TGA curves for various samples of POF-A system

TGA curves are shown in Fig. 6 and sub-systems A-2 was found to demonstrate the highest thermal resistance with a char yield of 51% at 600 ^{o}C (Table 4). All the samples in system-A were completely oxidized at 800 ^{o}C (Fig. 6).

These thermograms showed a high stability of POFs imparted by their unique microstructural features based on the relative balance of monomers.

In this context, thermal resistance of POFs was attributed to the presence of aromatic rings incorporated in the 3-D network of polyamide chains which is in accordance with the FTIR results.

Table 4 Thermal profile of different POFs

POF Sample	$^{a}T_{10}$ (^{o}C)	$^{b}T_{50}$ (^{o}C)	$^{c}\%Y_{C}$ (600^{o}C)
A-1	157	552	38
A-2	196	609	51
A-3	126	365	12

.

$^{a}T_{10}$: Temperature at 10% weight loss
$^{b}T_{50}$: Temperature at 50% weight loss
$^{c}\%Y_{C}$: Char yield or residual mass at 600 ^{o}C

E. BET Analysis

BET studies were performed in a TriStar II 3020 Version 2.00 Unit 1 Port 1. N_2 gas was employed as analysis adsorptive at 77K. Equilibration interval was set to 6s and weighed amount of dried A-3 sample was poured onto sample holder and evacuated for 6 hours for degassing purpose. A-3 showed BET surface area of 0.6503 m^2/g, average pore size of 32.8 nm and pore volume of 0.005 cm^3/g. The N_2 isoherms of A-3 (Fig. 7) demonstrate a Type-II behavior that is characteristic of macroporous architecture.

Adsorption is a strong function of microstructural features of POFs containing amide bonds. The internally decorated surfaces of various samples of POFs bearing multiple end functional groups such as $–NH_2$ and –COOH provide additional sites for the adsorption of gas molecules.

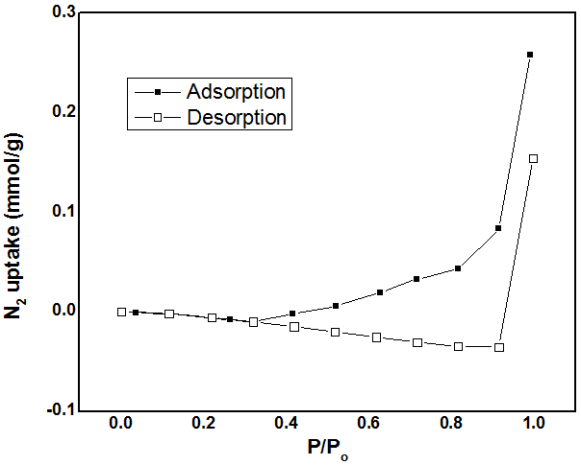

Fig. 7. N_2 isotherms for A-3 measured at 77K

Sub-systems A-1, A-2 and A-3 were decorated internally with amide linkages and externally with $–NH_2$ and –COOH end functional groups. These end functionalities possess significant affinity for gases like CO_2 and can provide adsorption sites for efficient CO_2 uptake. The surfaces with amine functional groups have been reported to offer sorption capabilities in ambient moisture [13-17]. Hence, these POF systems can be optimized for gas capture applications.

IV. Conclusion

Successful synthesis of POFs, bearing amides moieties and pendant functional groups, via an uncatalysed, one-step, metal free facile strategy was demostrated. Three POF sub-systems have been explored with the aim to optimize the pendant functional groups, thermal stability and morphology. In this regard, the relative molar concentrations of reacting species was selected as the major factor to tune the morphology and end reacticvity. Thus, by varying the molar concentrations quite distinct morphologies have been attained in POF sub-systems i.e. A-1, A-2 and A-3. These POFs were stable at 650 ^oC and maiantain their identity upto 800 ^oC. However, these POFs can be optimized further for their porosity control to find applications in gas selective adsorption, catalysis and H_2 storage in fuel cells.

References

[1] Han, S. S., Mendoza-Cortes, J. L., & Goddard, W. A. “Recent advances on simulation and theory of hydrogen storage in metal-organic frameworks and covalent organic frameworks”. Chemical Society Reviews, vol. 38, pp. 1460–76, 2009.

[2] Han, S. S., Furukawa, H., Yaghi, O. M., & Goddard, W. A. “Covalent Organic Frameworks as Exceptional Hydrogen Storage Materials”. Journal of the American Chemical Society, vol. 130, pp. 11580-11581, 2008.

[3] Wu, D., Xu, F., Sun, B., Fu, R., He, H., & Matyjaszewski, K. “Design and Preparation of Porous Polymers”. Chemical Reviews, vol. 112, pp. 3959-4015, 2012.

[4] Chang, Z., Zhang, D. -S., Chen, Q., & Bu, X. -H. “Microporous organic polymers for gas storage and separation applications”. Physical Chemistry Chemical Physics, vol. 15, pp. 5430-5442, 2013.

[5] Dawson, R., Cooper, A. I., & Adams, D. J. “Nanoporous organic polymer networks”. Progress in Polymer Science, vol. 37, pp. 530-563, 2012.

[6] Germain, J., Fréchet, J. M. J., & Svec, F. “Nanoporous Polymers for Hydrogen Storage”. Small, vol. 5, pp. 1098–1111, 2009.

[7] Wood, C, D., Tan, B., Trewin, A., Niu, H., Bradshaw, D., Rosseinsky, M. J., Khimyak, Y. Z., Campbell, N.L., Kirk, R., Stockel, E., & Cooper, A. I. “Hydrogen storage in microporous hypercrosslinked organic polymer networks”. Chemistry of Materials, American Chemical Society, vol. 19, pp. 2034–2048, 2007.

[8] Ferey, G., Serre, C., Devic, T., Maurin, G., Jobic, H., Llewellyn, P. L., & Chang, J. S. “Why hybrid porous solids capture greenhouse gases?”. Chemical Society Reviews, vol. 40, pp. 550-562, 2011.

[9] Liu, Y., Wu, S., Wang, G., Yu, G., Guan, J., Pan, C., & Wang, Z. “Control of porosity of novel carbazole-modified polytriazine frameworks for highly selective separation of CO_2-N_2”. Journal of Materials Chemistry A, vol. **2**, pp. 7795-7801, 2014.

[10] Msayib, K. J., Book, D., Budd, P. M., Chaukura, N., Harris, K. D. M., Helliwell, M., & McKeown, N. B. “Nitrogen and Hydrogen Adsorption by an Organic Microporous Crystal”. Angewandte Chemie International Edition, vol. 48, pp. 3273-3277, 2009.

[11] Mayr, B., Holzl, G., Eder, K., Buchmeiser, M. R., & Huber, C. G. “Hydrophobic, Pellicular, Monolithic Capillary Columns Based on Cross-Linked Polynorbornene for Biopolymer Separations”. Analytical Chemistry, vol. 74, pp. 6080-6087, 2002.

[12] Sinner, F., & Buchmeiser, M. R. “A New Class of Continuous Polymer Supports Prepared by Ring-Opening Metathesis Polymerization: A Straightforward Route to Functionalized Monoliths”. Macromolecules, vol. 33, pp. 5777-5786, 2000.

[13] Kizzie, A. C., Wong-Foy, A. G., & Matzger, A. J. “Effect of Humidity on the Performance of Microporous Coordination Polymers as Adsorbents for CO_2 Capture”. Langmuir, vol. 27, pp. 6368- 6373, 2011.

[14] Belmabkhout, Y., Serna-Guerrero, R., & Sayari, A. “Amine bearing mesoporous silica for CO_2 removal from dry and humid air”. Chemical Engineering Science, vol. 65, pp. 3695-3698, 2010.

[15] Choi, S., Drese, J. H., Eisenberger, P. M., & Jones, C. W. “Application of Amine-Tethered Solid Sorbents for Direct CO_2 Capture from the Ambient Air”. Environmental Science & Technology, vol. 45, pp. 2420-2427, 2011.

[16] Serna-Guerrero, R., Belmabkhout, Y., & Sayari, A. “Triamine grafted pore-expanded mesoporous silica for CO_2 capture: Effect of moisture and adsorbent regeneration strategies”. Adsorption, vol. 16, pp. 567-575, 2010.

[17] Sayari, A., & Belmabkhout, Y. “Amine-containing CO_2 adsorbents: dramatic effect of water vapor”. Journal of American Chemical Society, vol. 132, pp. 6312-6314, 2010.